ACS NANO

www.acsnano.org

ARTICLE

# Reversible and Precise Self-Assembly of Janus Metal-Organosilica Nanoparticles through a Linker-Free Approach

Huicheng Hu,[†,‡] Fei Ji,[†,‡] Yong Xu,[†,‡] Jiaqi Yu,[†] Qipeng Liu,[†] Lei Chen,[†] Qian Chen,[§] Peng Wen,[†] Yeshayahu Lifshitz,[*,†,⊥] Yan Wang,[∥] Qiao Zhang,[*,†] and Shuit-Tong Lee[*,†]

[†]Institute of Functional Nano & Soft Materials (FUNSOM), Collaborative Innovation Center of Suzhou Nano Science and Technology (NANO-CIC), Jiangsu Key Laboratory for Carbon-Based Functional Materials & Devices, Soochow University, Suzhou, Jiangsu 215123, P. R. China

[⊥]Department of Materials Science and Engineering, Technion - Israel Institute of Technology, Haifa 3200003, Israel

[§]Department of Materials Science and Engineering, University of Illinois at Urbana−Champaign, 104 South Goodwin Ave, Urbana, Illinois 61801, United States

[∥]Institute of Environment and Sustainable Development in Agriculture, Chinese Academy of Agricultural Sciences, No. 12 South Street of Zhongguancun Haidian District, Beijing 100081, China

Supporting Information

**ABSTRACT:** **Reversible self-assembly of nanoparticles into ordered structures is essential for both fundamental study and practical applications. Although extensive work has been conducted, the demand for simple, cheap, reversible, and versatile ordering methods is still a central issue in current nanoscience and nanotechnology. Here we report a reversible and precise self-assembly of nanoparticles through a linker-free and fast approach by manipulating the interparticle forces, *e.g.*, van der Waals (VDW) force and electrostatic force. Because VDW force is nondirectional, an oriented interaction is achieved to induce the directional binding of nanoparticles utilizing the Janus nanostructure. An effective sol−gel approach has been developed to synthesize metal-organosilica Janus nanoparticles. Dimers and trimers can be obtained by tuning the steric hindrance. After assembly, "hot-spots" can be generated between adjacent nanoparticles, and dramatic enhancement has been observed in surface-enhanced Raman scattering. The present strategy overcomes several limitations of existing approaches and allows the controlled assembly of small particles into various structures.**

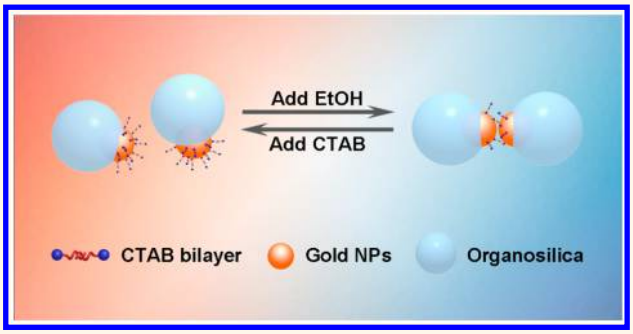


**KEYWORDS:** *reversible self-assembly, Janus nanoparticle, van der Waals force, surface-enhanced raman spectroscopy, surface plasmon resonance*

Self-assembly of nanoparticles into functional structures has been regarded as a powerful bottom-up approach that can produce new materials,[1−8] especially metamaterials, with fascinating properties for sensing,[9,10] optoelectronic devices,[11] catalysis,[12] color printing,[13] surface-enhanced Raman spectroscopy (SERS),[14−16] and so on. Among various self-assembly approaches, the reversible self-assembly that can assemble and disassemble nanoparticles upon external stimuli, such as temperature,[17,18] pH,[19,20] light,[21−24] and magnetic field,[25,26] is of special interest because of their potential applications in photoswitchable catalysis,[27] remote controlled intracellular signaling,[28] circular dichroism device,[29] precise drug delivery,[7] and smart materials.[30] Despite the extensive research on reversible self-assembly, there are still several challenges. For example, linkers are required in most of the reported approaches to connect nanoparticles. Although a number of linkers, such as polypeptide, polyrotaxane, spiropyran, and DNA, have been reported,[31−36] they usually suffer from high cost, tedious preparation process, and low stability and adaptability under intricate chemical and biological environments. More importantly, it remains a great challenge to precisely control the aggregation of nanoparticles, and some reported approaches can produce only random aggregates of nanoparticles.

Received: May 23, 2016
Accepted: July 8, 2016
Published: July 8, 2016





DOI: 10.1021/acsnano.6b03396
*ACS Nano* 2016, 10, 7323−7330

According to the Derjaguin–Landau–Verwey–Overbeek (DLVO) theory, colloidal nanoparticles are separated from each other by repulsive force, e.g., electrostatic repulsion force; otherwise, they will aggregate due to the van der Waals (VDW) attraction force. Although it is straightforward to assemble nanoparticles by manipulating the interparticle forces, it is difficult to realize the reversible and precise self-assembly.[37] For example, because VDW force is a nondirectional force and mainly depends on the intrinsic properties of materials, one may obtain only random aggregates. A possible approach to achieve precise control is to utilize the Janus or "patchy" nanoparticles,[38] in which an oriented interaction can be introduced into the system. The resulting anisotropic interactions can mimic the directional bonds of atomic systems and produce the potential assembly in a controllable manner, although it is difficult to make well-defined Janus nanoparticles on demand. Additionally, when nanoparticles get in close contact, the net potential is predicted to approach negative infinity, and the particles will fuse together,[39,40] preventing the disassembly process. In this work, we present a versatile strategy to realize the reversible and linker-free self-assembly of Janus nanoparticles in a precise and fast manner. By taking advantage of the weak interaction between the capping ligand and metal surface, Janus Au-organosilica nanoparticles can be assembled into dimers or trimers when the nanoparticles are dispersed in ethanol. The formation of dimers or trimers is mainly determined by the size ratio between Au nanoparticle and organosilica. The assembled nanostructures can be readily disassembled when they are redispersed into hexadecyltrimethylammonium bromide (CTAB) aqueous solution upon ultrasonication. We believe this precise and reversible approach will shed some light on self-assembly design.

## RESULTS AND DISCUSSION

The approach we propose to directionally assemble the Au nanoparticles is schematically illustrated in Scheme 1. CTAB bilayer capped Janus Au-organosilica nanoparticles were synthesized and used as the building blocks. This anisotropic structure takes advantage of different VDW attraction forces between metals (such as Au, Ag, and Pd) and oxides (such as organosilica). Since the Hamaker constants of metal–metal are much larger than those of oxide–oxide,[39] the VDW forces of the as-synthesized Janus Au-organosilica nanoparticles distribute unevenly and result in an oriented interaction possessing directionality. Most CTAB molecules bonded to AuNPs can be easily removed when the Janus nanoparticles are dispersed in ethanol because the interaction between CTAB bilayer and gold surface is relatively weak. The organosilica possesses a stronger interaction with CTAB than Au nanoparticle because CATB molecules are used as the templates to anisotropically grow organosilica (Supplementary Figure S1), and only under very harsh chemical environment, e.g., refluxing in acidic condition for 24 h, can these CTAB molecules be removed.[41,42] As a result, the addition of ethanol can trigger the self-assembly process. Meanwhile, since CTAB molecules on the surface of Au nanoparticle are not completely removed, the remaining CTAB surfactants exert short-range steric repulsion which counteracts the attractive force between Au nanoparticles and thus enables reversible disassembly of Au nanoparticles under ultrasonication in CTAB aqueous solution.

**Scheme 1. Schematic Illustration of the Reversible Self-Assembly of Janus Au-Organosilica Nanoparticles**[a]

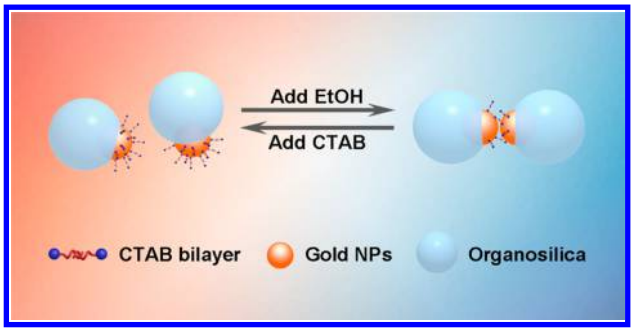


[a]Upon addition of ethanol, most CTAB molecules on gold surface were removed, triggering the assembly of Janus nanoparticles. When excessive CTAB aqueous solution was added to the aggregates, the aggregates can be disassembled under ultrasonication.

Figure 1a–c shows the TEM images of one complete cycle of the assembly and disassembly of Janus Au-organosilica nanostructure. To obtain the designed Janus nanoparticle, we developed a sol–gel approach, in which CTAB-capped Au nanoparticles were mixed with 1,2-bis(triethoxysilyl)ethane (BTEE), water, ethanol, and ammonia. The precursor of organosilica, BTEE, is apt to anisotropically polymerize on the surface of Au nanoparticles because of the negative total surface energy ($\Delta\sigma = \sigma_{\text{organosilica-solvent}} + \sigma_{\text{organosilica-core}} - \sigma_{\text{core-solvent}} < 0$), leading to the Volmer–Weber island growth mode.[42] TEM and SEM images (Supplementary Figures S1 and S2) show clearly the anisotropic morphology evolution of organosilica and the final Janus geometry. Monodisperse Janus Au-organosilica nanoparticles with almost 100% yield were synthesized. Distributions of different elements, including oxygen (O), silicon (Si), and gold (Au) from the elemental mapping further confirmed the Janus nanostructure (Supplementary Figure S3). Some AuNPs were coated with a very thin layer of silica (~1–2 nm in thickness). To ensure the exposure of Au surface, an additional regrowth process was conducted, as described in the Methods section. The average size of Au nanoparticles and organosilica is approximately 44 and 120 nm, respectively (Figure 1a). Upon adding ethanol solution, CTAB molecules on the surface of Au nanoparticles were removed, and the Janus nanoparticles dimerized immediately, indicated by the color change from ruby red to purple (the inset in Figure 1b, also see the video in the Supporting Information). The assembly process can be completed within several seconds, which is much quicker than those methods using various linkers that take at least several hours.[21] Magnified TEM image of one individual dimer is shown at the top right. According to our counts based on more than 300 nanoparticles from TEM images, the proportion of dimer (defined as the number of dimerized nanoparticles divided by total number of nanoparticles) reached approximately 70.0%. It is worth pointing out that no purification process has been conducted and the self-assembly process can be carried out in a large scale (as large as 1L scale), suggesting this assembly process is a promising method. The density difference of residual CTAB on the surface of Au and organosilica has been confirmed by the elemental mapping and energy-dispersive X-ray (EDX) data (Supplementary Figure S4). After transferring back to the CTAB aqueous solution and treating with ultrasonication, dimers were disassembled and well dispersed in solutions again, as evidenced by both the TEM image (Figure 1c), and the solution color changed from purple to red (inset in Figure 1c).


DOI: 10.1021/acsnano.6b03396
ACS Nano 2016, 10, 7323–7330

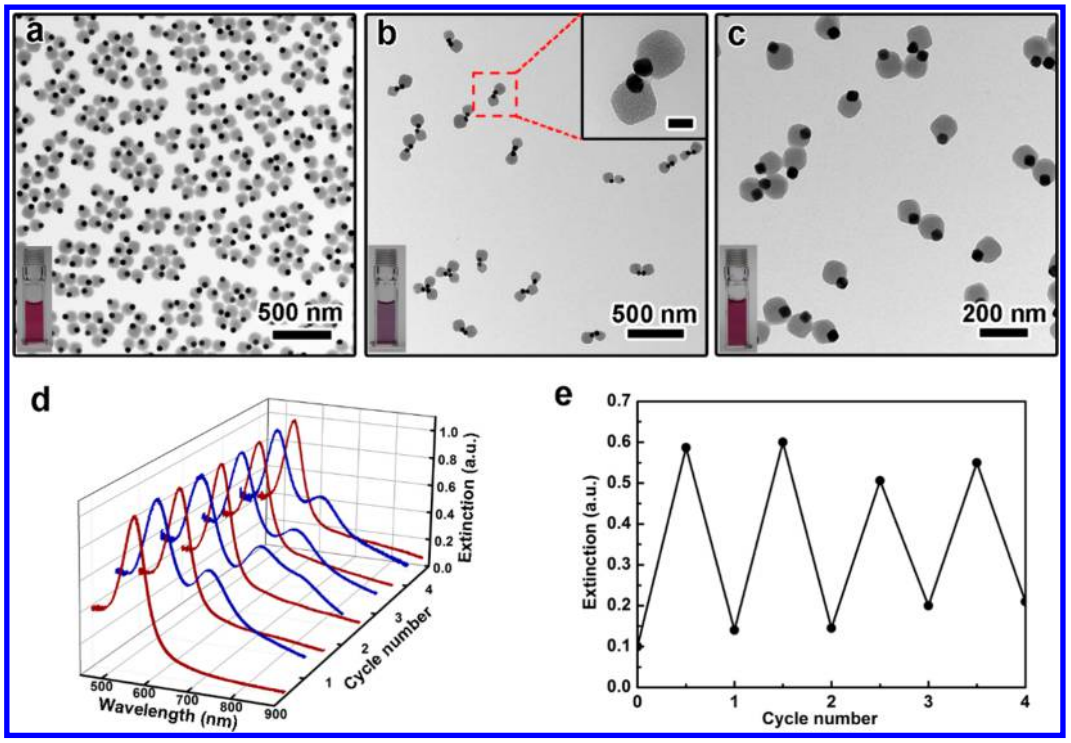


**Figure 1.** (a–c) TEM and photographs of samples: (a) original, (b) self-assembled, and (c) disassembled Janus NPs. The scale bar of the inset in (b) is 50 nm. (d) 3D UV–vis spectra of four completed cycles containing disassembled NPs (red line) and assembled NPs (blue line). (e) The repeated switching of the intensity of the second peak for four cycles.

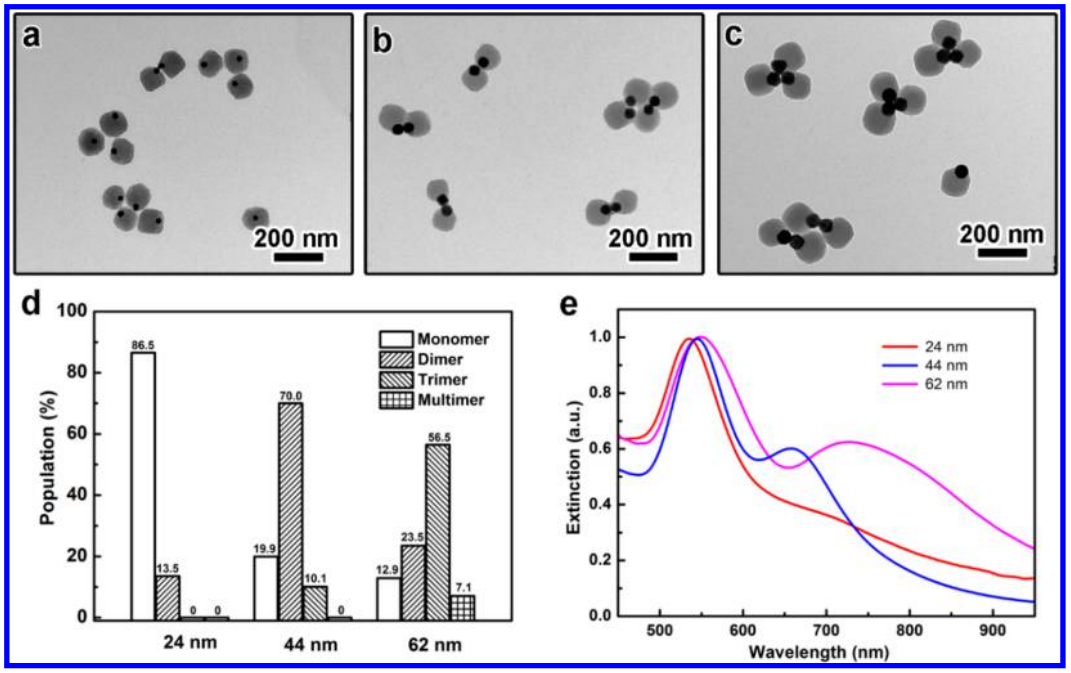


**Figure 2.** (a–c) TEM characterization of assembled NPs with different steric hindrance. The size of Au NPs is (a) 24, (b) 44, and (c) 62 nm. The size of organosilica is fixed at about 120 nm. (d) Statistical analysis of the product distribution with different steric hindrance. (e) Normalized UV–vis spectra of assembled NPs with different steric hindrance.

As a comparison, when Au nanoparticles capped with CTAB molecules were dispersed into ethanol, only irreversible and irregular aggregates were observed (Supplementary Figure S5).

To investigate the reversibility and stability of this assembly process, four cycles of reversible assembly were demonstrated, and the corresponding UV–vis spectra are shown in Figure 1d. The intrinsic plasmonic peak of the Au-organosilica composite is at around 530 nm, resulting from the localized surface plasmon resonance effect of Au nanoparticles. After assembly, a distinct peak at about 670 nm was observed, and the position of the intrinsic or first peak did not change. The new or second peak resulted from the plasmonic coupling between Au nanoparticles, suggesting the formation of aggregates.[43] During the assembly and disassembly process, the second extinction



DOI: 10.1021/acsnano.6b03396
ACS Nano 2016, 10, 7323–7330

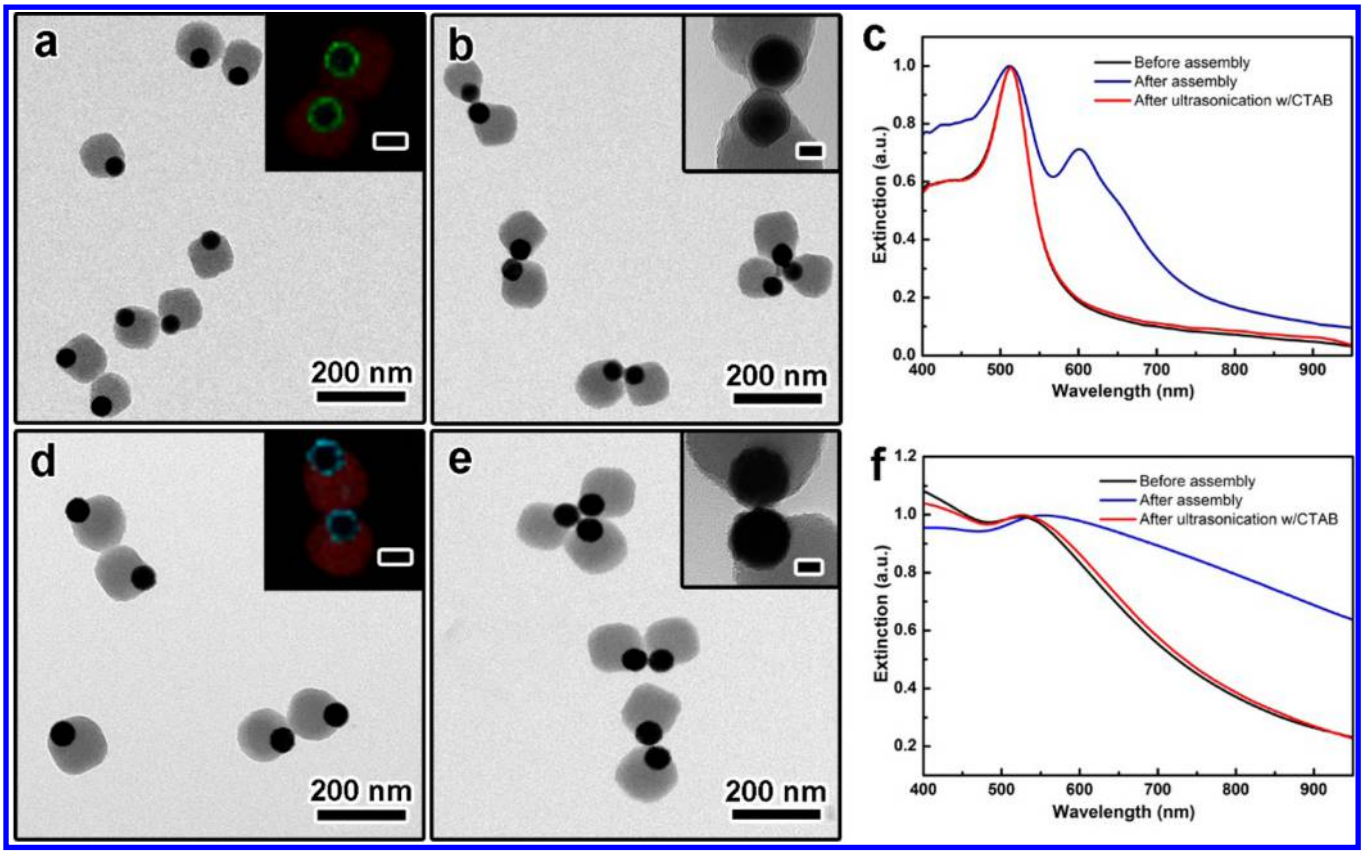


**Figure 3. (a, b, d, e) TEM characterization of (a) original and (b) assembled Janus Au@Ag-organosilica NPs; (d) original Janus; and (e) assembled Au@Pd-organosilica NPs. The insets in (a) and (d) show the overlaid elemental mapping images. The scale bars in the inset of (a, d) are 50 nm. The scale bars in the inset of (b, e) are 20 nm. (c, f) Normalized UV−vis spectra of (c) Au@Ag-organosilica NPs and (f) Au@Pd-organosilica NPs before assembly (black line), after assembly (blue line), and after ultrasonication with CTAB (red line).**

peak would emerge and disappear, respectively, corresponding to the solution color switching between red and purple. To illustrate the reversibility and stability of this system more clearly, Figure 1e shows the fairly constant intensity of the second peak in four cycles, indicating the nanoparticles are still in good states after four cycles. It is worth pointing out that these dimers can also be fixed by silica coating (Supplementary Figure S6).

Steric hindrance plays an important role here in the precise self-assembly of Janus nanoparticles, which can be manipulated by tuning the ratio between the size of Au nanoparticle and the size of organosilica. Theoretically, with the increase of Au nanoparticle size, the proportion of Au nanoparticles exposed in solution will increase, which causes a greater possibility for Au nanoparticles to be in contact with each other, leading to a higher yield of dimerization. On the other hand, when the exposed surface area of Au nanoparticles increases, each Au nanoparticle can come into contact with more nanoparticles, leading to the formation of trimers or even quatermers. To confirm this hypothesis, Au nanoparticles with three different sizes, 24, 44, and 62 nm, were synthesized and used as the building units, while the size of organosilica was kept constant at about 120 nm. As shown in Figure 2a−c, increasing Au nanoparticle size leads to more assembled nanostructures. At the same time, Figure 2b,c shows clearly the proportion of trimers raised obviously. To have a more accurate analysis on the population of different constitutes, statistics of each sample based on more than 300 counts were conducted (Figure 2d). When the size of Au nanoparticles was about 24 nm, the products were composed of 86.5% single Janus nanocomposite and 13.5% dimers. No trimers or quatermers have been observed. As the size of Au nanoparticles increased to ∼44 nm, the proportion of dimers approached ∼70.0%, while trimers started to emerge and accounted for ∼10.1%. With a further increase of Au nanoparticles size to 62 nm, the proportion of trimers increased to ∼56.5% and some quatermers (about 7.1%) can also be found. UV−vis spectra provided another perspective on this evolution process (Figure 2e). The slight redshift of the first plasmonic peak at around 530 nm can be explained by multipole scattering theory.[44] For the second peak, a shoulder started to develop in the longer wavelength when the size of AuNPs was ∼24 nm, indicating a small amount of assembled aggregates. With larger particle size, a distinct peak at ∼670 nm emerged due to a higher degree of dimerization. Finally, this peak red-shifted to ∼725 nm because of the trimerization of nanoparticles, while the shoulder at longer wavelength can be ascribed to the plasmonic coupling of quatermers (Supplementary Figure S8).

In previous reported self-assembly methods utilizing cross-linked molecules as the linkers,[32,35] the bonding selectivity between molecular linkers and nanoparticles cannot be neglected, which often limits the versatility of those approaches. Since the VDW attraction force is universal, the method reported in this research may be applied to various metal materials. Silver (Ag) and palladium (Pd) are demonstrated here to prove the versatility of this approach. To clearly monitor the assembly process, Au@Ag and Au@Pd core−shell nanoparticles are used because the plasmonic property of Au



DOI: 10.1021/acsnano.6b03396
ACS Nano 2016, 10, 7323−7330

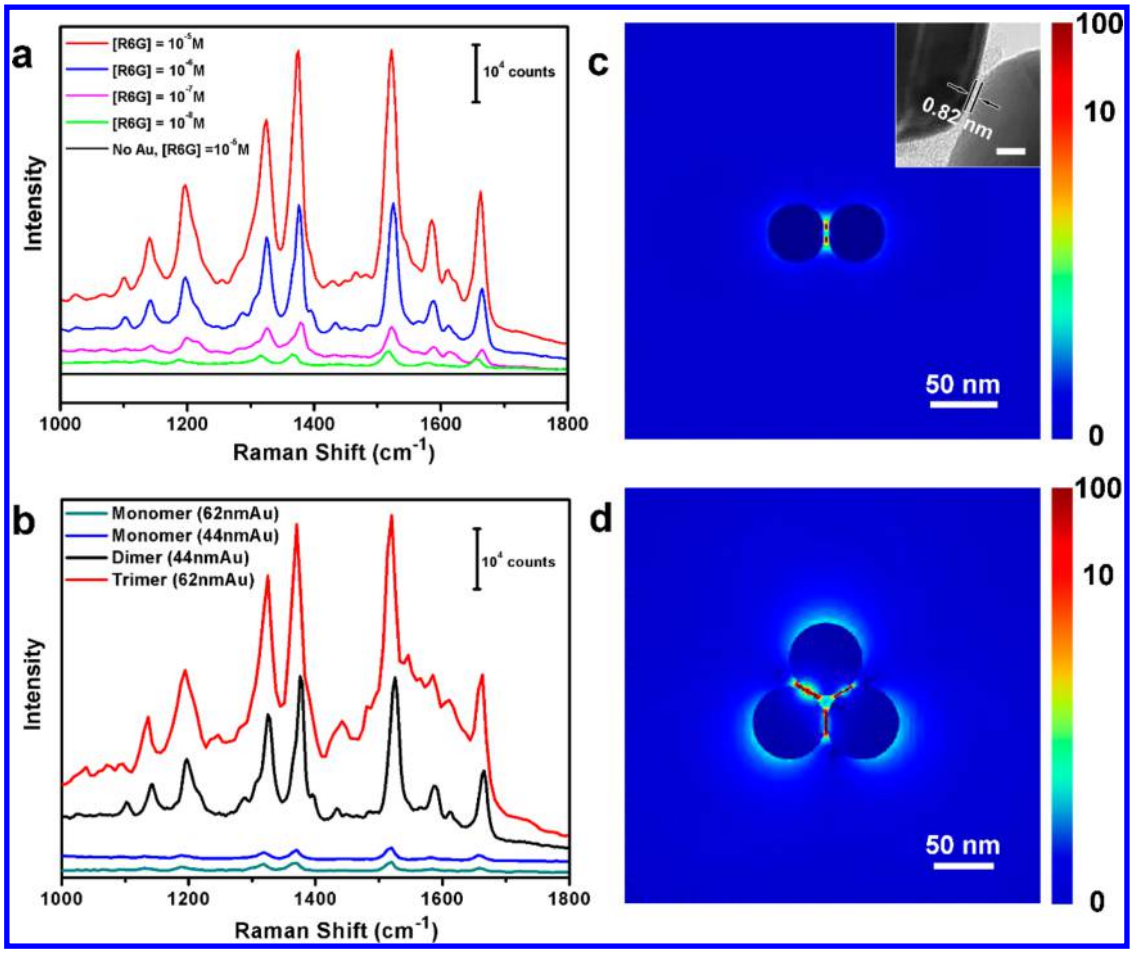


**Figure 4. (a) Raman spectra of R6G with different concentration adsorbed on assembled Au-organosilica dimers. Black line is the Raman spectra of R6G ([R6G] = $10^{-5}$ M) on naked substrate. (b) Comparison of SERS performance before and after self-assembly. The concentration of R6G is $10^{-6}$ M. Incident laser excitation wavelengths in both (a) and (b) are 633 nm. (c) Localized electromagnetic field distributions of dimer. The inset shows a magnified TEM image of a dimer. The scale bar in the inset of (c) is 5 nm. (d) Localized electromagnetic field distributions of a trimer.**

can make the process more vivid. Janus Au@Ag-organosilica and Au@Pd-organosilica nanocomposite were synthesized by regrowth of Ag and Pd on Au-organosilica nanostructure, respectively (Figure 3a,d). After transferring into an ethanol solution, the assembly process was triggered (Figure 3b, 3e). The elemental mapping image in the insets shows clearly that Ag and Pd did grow on the Au nanoparticles. Figure 3c shows the UV−vis spectra of one cycle for the assembly and disassembly process of Au@Ag-organosilica nanoparticles. The original Janus nanoparticles showed a sharp peak at 505 nm, further confirming the formation of Au@Ag core−shell nanostructure.[45] After assembly, a longitudinal plasmonic coupling peak appeared at 610 nm, which is similar to Au-organosilica dimers. After ultrasonication treatment in the presence of excessive CTAB molecules, the second peak disappeared, and the spectrum returned to almost the same spectrum before assembly. Figure 3f shows the UV−vis spectra of one cycle for the reversible self-assembly of Au@Pd-organosilica. It is clear that the plasmonic peak of the Au core dampened with the formation of the Pd shell, which can be attributed to the significantly smaller conductivity of Pd than Au at optical frequency.[46] As a result, only a broad shoulder can be observed after assembly, which disappeared and returned to almost the same spectrum after ultrasonication treatment with excessive CTAB.

The ability to precisely organize Au nanoparticle into dimers or trimers allows us to take full advantage of the near-field coupling for application in SERS. It is well-known that SERS activity of noble metal depends not only on its intrinsic properties but also on the particle shape, size, and interparticle distance. When two neighboring metallic nanoparticles are illuminated, an intense electromagnetic field, so-called "hot-spots", can appear.[47,48] In this work, rhodamine 6G (R6G) molecules were used as probe molecules. As shown in Figure 4a, no signal was detected when naked silicon slice (without any Janus nanoparticles) was used as substrate ([R6G] = $10^{-5}$ M). When the assembled nanoparticles were deposited on the silicon substrate, characteristic peaks from 1000 to 1800 $cm^{-1}$ were observed clearly. A signal can still be detected even when the concentration of R6G solutions was diluted to $10^{-8}$ M. As a comparison, the SERS performance of monomers before assembly was also investigated. The same amount of Janus nanoparticles was deposited on to the substrate ([R6G] = $10^{-6}$ M). As shown in Figure 4b, impressive enhancement of assembled nanoparticles was obtained under the same condition, further confirming the hot-spots effect. The enhancement factor (EF) of Au-organosilica (the size of AuNPs is 44 nm) is around $5.1 \times 10^5$, and the EF of the corresponding dimers is about $6.6 \times 10^6$, giving a ~ 13 times enhancement. The EF of trimers is about $1.6 \times 10^7$, which is



DOI: 10.1021/acsnano.6b03396
ACS Nano 2016, 10, 7323−7330

about 31 times higher than that of monomers. If the hot-spot is assumed to constitute 1/100 of the total NP surface (*i.e.*, 60 $nm^2$ for 44 nm AuNPs and 120 $nm^2$ for 62 nm AuNPs), then each dimeric hotspot would be 650 times as strong as a monomer and each trimeric hot-spot 1275 times as strong per unit area.[43]

To investigate the possible contribution to this enhancement, spatial distributions of electromagnetic field intensity of a dimer (Figure 4c) and a trimer (Figure 4d) were calculated using the finite-difference time-domain (FDTD) method. The gap widths between two neighboring nanoparticles fell into a narrow range of ~0.7−0.9 nm, further confirming that short-range repulsion forces do exist when Au nanoparticles contact and enable the reversible process. Highly concentrated plasmonic hot-spots between two neighboring nanoparticles occurred around the gap which ensured a strong electromagnetic field for SERS enhancement. This result is in good agreement with theoretical predictions. Finally, a more vivid demonstration of the reversible self-assembly process was displayed using a special pattern engraved PDMS gel (the area is 18.5 cm × 7.2 cm, Supplementary Figure S11). As shown in Figure S12, the original color of the solution is ruby red, which turned to purple when the self-assembly process was triggered. After treated with ultrasonication in CTAB solution, the color turned back into red again.

## CONCLUSIONS

We have presented a reversible and precisely controllable self-assembly of nanoparticles through a fast and linker-free approach by manipulating the interparticle forces and steric hindrance. An oriented interaction is achieved by forming a metal-organosilica Janus nanostructure. When the surface charge was decreased by washing the Janus nanostructure with ethanol, the balance between van der Waals force and electrostatic repulsion was broken, resulting in the self-assembly of Janus nanoparticles. Thanks to the short-range steric repulsion force derived from the remaining CTAB ligands, the reversible process can be easily realized when the surface charge recovered by treating with CTAB solution under ultrasonication. High-yield dimers or trimers can be obtained in solution and produced in large scale by tuning the steric hindrance. The present approach is not just linker-free but also cheap, simple, reversible, and versatile (was demonstrated for three types of nanoparticles). This method *via* manipulation of interparticle forces and steric hindrance provides another perspective in the future design of reversible and precisely controllable self-assembly of nanoparticles.

## METHODS

**Materials.** Gold(III) chloride trihydrate ($HAuCl_4 \cdot 3H_2O$, ≥49.0% Au basis), L-ascorbic acid (AA assay: 99.7−100.5%), sodium hydroxide (NaOH, AR, ≥ 96%), 1,2-bis(triethoxysilyl)ethane (BTEE, 96%), and tetraethyl orthosilicate (TEOS, 99.9%) were purchased from Sigma-Aldrich. Hexadecyltrimethylammonium chloride (CTAC, >95.0%) and hexadecyltrimethylammonium bromide (CTAB, >98.0%) were purchased from TCI. Ammonia aqueous solution (28 wt %) was purchased from Aladdin. Rhodamine 6G (R6G) was purchased from Sinopharm. Milli-Q water with a resistivity >18.0 MΩ·cm was used in the preparation of aqueous solutions. All glassware was cleaned with aqua regia ($V_{HCl}$:$V_{HNO_3}$ = 3:1) and then washed with large amounts of Milli-Q water. All the chemical reagents were used as received without further purification.

**Characterization.** TEM data were collected at 200 kV on a TECNAI G2 F20 from FEI, USA. SEM data were collected at 5 kV using Zeiss Supra55 from Carl Zeiss, Germany. All the UV−vis spectra were recorded in a range of 300−1050 nm by using the LAMBDA 750 spectrograph from Perkin Elmer, U.S.A. All the Raman spectra were recorded on a Jobin Yvon Raman confocal system (HR800) equipped with an integral light microscope (Olympus) with a 50× objective.

**Au NPs Synthesis.** Au nanoparticles were prepared by a ascorbic acid (AA) reduction procedure similar to the method reported by Zheng *et al.*[49] First, 20 nm diameter gold nanoparticles were synthesized with the method reported before.[50] The product was centrifuged at 11000 rpm for 15 min and then dispersed into 6 mL CTAB solution (75 mM) solution. Aqueous $HAuCl_4$ solution (0.01 M, 0−10 mL) was added dropwise (*ca.* 2 mL/h) by a syringe pump into a 100 mL conical flask containing aqueous CTAB solution (0.04 M, 40 mL), AA solution (0.1 M, 0−3 mL), and 2 mL gold nanoparticles solution synthesized above with vigorous stirring. Finally Au NPs with different diameters ranging from ~20 to ~70 nm were obtained, and the product was centrifuged at 11000−6500 rpm for 15 min and dispersed into 2 mL aqueous CTAB solution (75 mM).

**Janus Au-Organosilica NPs Synthesis.** Typically, 2 mL CTAB-capped Au NPs solution prepared above was added to a mixed solution containing 20.5 mL Milli-Q water, 1.5 mL ethanol, and 0.55 mL ammonia solution (28 wt %). After stirring for 30 min, 30 μL BTEE was quickly injected with continuous stirring. After 4 h reaction in room temperature, the product was centrifuged at 8000 rpm for 10 min, washed with ethanol once, and dispersed into 5 mL ethanol at last. To ensure the exposure of Au surface, a regrowth process was carried out. Aqueous $HAuCl_4$ solution (25 mM, 1.5 mL) was added dropwise (*ca.* 6 mL/h) by a syringe pump into a 50 mL conical flask containing aqueous CTAB solution (0.04 M, 20 mL), AA solution (0.1 M, 0.3 mL), and 1 mL CTAB-capped Janus nanoparticles solution with vigorous stirring. The product was centrifuged at 8000 rpm for 10 min and dispersed in water.

**Self-Assembly.** *Self-Assembly of Janus Au-Organosilica NPs.* To trigger the self-assembly process, a certain amount of ethanol was added to the aqueous solution containing Janus nanoparticles. To disassemble the nanoparticles, the aggregates were centrifuged and redisposed into CTAB solution (100 mM) under ultrasonication.

*Self-Assembly of Janus Au@Pd-Organosilica NPs.* Aqueous $Na_2PdCl_4$ solution (25 mM, 1.5 mL) was added dropwise (*ca.* 6 mL/h) into a 50 mL conical flask containing aqueous CTAB solution (0.04 M, 20 mL), AA solution (0.1 M, 0.3 mL), and 1 mL CTAB-capped Janus nanoparticles solution with vigorous stirring. The product was centrifuged at 8000 rpm for 10 min and dispersed in water. To trigger the self-assembly process, a certain amount of ethanol was added to the solution. To disassemble the nanoparticles, the aggregates were centrifuged and redisposed into CTAB solution (100 mM) under ultrasonication.

*Self-Assembly of Janus Au@Ag-Organosilica NPs.* Aqueous $AgNO_3$ solution (25 mM, 1.5 mL) was added dropwise (*ca.* 6 mL/h) into a 25 mL conical flask containing aqueous CTAC solution (0.02 M, 10 mL) and 1 mL CTAB-capped Janus nanoparticles solution by a syringe pump. Another aqueous solutions containing CTAC (0.08 M, 1 mL) and AA (0.1M, 1 mL) was added into the conical flask dropwise (*ca.* 6 mL/h) using a syringe pump simultaneously. The reaction proceeded under 60 °C hot water bath with vigorous stirring. The product was centrifuged at 8000 rpm for 10 min and dispersed in water. To trigger the self-assembly process, a certain amount of ethanol was added to the solution. To disassemble the nanoparticles, the aggregates were centrifuged and redisposed into CTAB solution (100 mM) under ultrasonication.

**SERS Experiments.** The SERS performance of the product was tested using R6G as the probe molecule. The products were mixed with R6G solutions of different concentrations ($10^{-5}$ M, $10^{-6}$ M, $10^{-7}$ M, and $10^{-8}$ M). Then the mixed sample was distributed onto plasma-treated silicon slices and dried naturally. All the samples were irradiated with a laser with laser power of 0.6 mW (633 nm excitation) and an exposure time of 5 s.

**FDTD Simulations.** The simulation of localized electromagnetic field distributions was performed by a software package, FDTD Solution 8.0. The geometric parameters of the dimer and trimer were



DOI: 10.1021/acsnano.6b03396
ACS Nano 2016, 10, 7323−7330

consistent with TEM images. All the gap widths were set to 0.8 nm during simulation. Laser excitation wavelength was 670 nm for the dimer and 725 nm for the trimer, respectively. The refractive index of ethanol was taken to be 1.36 as background. The dielectric permittivity of gold was taken from previous reported work (Palik, E. D. *Handbook of Optical Constants of Solids*, Vol. 1; Academic Press, 1997). In this work, it should be noticed that a circularly polarized electromagnetic plane wave was launched to simulate the light interacting with the nanostructures. Furthermore, the simulation regions were divided into meshes of 0.5 nm in size.

## ASSOCIATED CONTENT

### Supporting Information

The Supporting Information is available free of charge on the ACS Publications website at DOI: 10.1021/acsnano.6b03396.

Additional TEM and SEM images and photographs (PDF)
(AVI)

## AUTHOR INFORMATION


### Corresponding Authors

*E-mail: shayli@tx.technion.ac.il.
*E-mail: qiaozhang@suda.edu.cn.
*E-mail: apannale@suda.edu.cn.

### Author Contributions

‡These authors contributed equally.


### Notes

The authors declare no competing financial interest.

## ACKNOWLEDGMENTS

We thank the financial support from the National Natural Science Foundation of China (21401135) and the Natural Science Foundation of Jiangsu Province (BK20140304). We also acknowledge the support from the Priority Academic Program Development of Jiangsu Higher Education Institutions (PAPD) and the Soochow University - Western University Centre (SWC) for Synchrotron Radiation Research. Y.X. acknowledges the Collaborative Innovation Center of Suzhou Nano Science and Technology (Nano-CIC) for the fellowship of "Collaborative Academic Training Program for Post-Doctoral Fellows".

## REFERENCES


(1) Whitesides, G. M.; Grzybowski, B. Self-Assembly at All Scales. *Science* **2002**, *295*, 2418−2421.
(2) Bharti, B.; Fameau, A. L.; Rubinstein, M.; Velev, O. D. Nanocapillarity-Mediated Magnetic Assembly of Nanoparticles into Ultraflexible Filaments and Reconfigurable Networks. *Nat. Mater.* **2015**, *14*, 1104−1109.
(3) Shevchenko, E. V.; Talapin, D. V.; Kotov, N. A.; O'Brien, S.; Murray, C. B. Structural Diversity in Binary Nanoparticle Superlattices. *Nature* **2006**, *439*, 55−59.
(4) Grzelczak, M.; Vermant, J.; Furst, E. M.; Liz-Marzán, L. M. Directed Self-Assembly of Nanoparticles. *ACS Nano* **2010**, *4*, 3591−3605.
(5) Lewandowski, W.; Fruhnert, M.; Mieczkowski, J.; Rockstuhl, C.; Gorecka, E. Dynamically Self-Assembled Silver Nanoparticles as a Thermally Tunable Metamaterial. *Nat. Commun.* **2015**, *6*, 6590.
(6) Nie, Z.; Petukhova, A.; Kumacheva, E. Properties and Emerging Applications of Self-Assembled Structures Made from Inorganic Nanoparticles. *Nat. Nanotechnol.* **2010**, *5*, 15−25.
(7) Ohta, S.; Glancy, D.; Chan, W. C. W. DNA-Controlled Dynamic Colloidal Nanoparticle Systems for Mediating Cellular Interaction. *Science* **2016**, *351*, 841−845.
(8) Tang, Z.; Kotov, N. A. One-Dimensional Assemblies of Nanoparticles: Preparation, Properties, and Promise. *Adv. Mater.* **2005**, *17*, 951−962.
(9) Lee, J.; Hernandez, P.; Lee, J.; Govorov, A. O.; Kotov, N. A. Exciton-Plasmon Interactions in Molecular Spring Assemblies of Nanowires and Wavelength-Based Protein Detection. *Nat. Mater.* **2007**, *6*, 291−295.
(10) Lee, J.-S.; Han, M. S.; Mirkin, C. A. Colorimetric Detection of Mercuric Ion ($Hg^{2+}$) in Aqueous Media Using DNA-Functionalized Gold Nanoparticles. *Angew. Chem.* **2007**, *119*, 4171−4174.
(11) Ozbay, E. Plasmonics: Merging Photonics and Electronics at Nanoscale Dimensions. *Science* **2006**, *311*, 189−193.
(12) Yao, Y.; Xue, M.; Zhang, Z.; Zhang, M.; Wang, Y.; Huang, F. Gold Nanoparticles Stabilized by an Amphiphilic Pillar[5]Arene: Preparation, Self-Assembly into Composite Microtubes in Water and Application in Green Catalysis. *Chem. Sci.* **2013**, *4*, 3667.
(13) Kim, H.; Ge, J.; Kim, J.; Choi, S.-E.; Lee, H.; Lee, H.; Park, W.; Yin, Y.; Kwon, S. Structural Colour Printing Using a Magnetically Tunable and Lithographically Fixable Photonic Crystal. *Nat. Photonics* **2009**, *3*, 534−540.
(14) Alvarez-Puebla, R.; Agarwal, A.; Manna, P.; Khanal, B.; Aldeanueva-Potel, P.; Carbó-Argibay, E.; Pazos-Pérez, N.; Vigderman, L.; Zubarev, E.; Kotov, N. Gold Nanorods 3d-Supercrystals as Surface Enhanced Raman Scattering Spectroscopy Substrates for the Rapid Detection of Scrambled Prions. *Proc. Natl. Acad. Sci. U. S. A.* **2011**, *108*, 8157−8161.
(15) Lee, Y. H.; Shi, W.; Lee, H. K.; Jiang, R.; Phang, I. Y.; Cui, Y.; Isa, L.; Yang, Y.; Wang, J.; Li, S.; Ling, X. Y. Nanoscale Surface Chemistry Directs the Tunable Assembly of Silver Octahedra into Three Two-Dimensional Plasmonic Superlattices. *Nat. Commun.* **2015**, *6*, 6990.
(16) Lim, D. K.; Jeon, K. S.; Hwang, J. H.; Kim, H.; Kwon, S.; Suh, Y. D.; Nam, J. M. Highly Uniform and Reproducible Surface-Enhanced Raman Scattering from DNA-Tailorable Nanoparticles with 1-Nm Interior Gap. *Nat. Nanotechnol.* **2011**, *6*, 452−460.
(17) Heo, K.; Miesch, C.; Emrick, T.; Hayward, R. C. Thermally Reversible Aggregation of Gold Nanoparticles in Polymer Nanocomposites through Hydrogen Bonding. *Nano Lett.* **2013**, *13*, 5297−5302.
(18) Liu, Y.; Han, X.; He, L.; Yin, Y. Thermoresponsive Assembly of Charged Gold Nanoparticles and Their Reversible Tuning of Plasmon Coupling. *Angew. Chem., Int. Ed.* **2012**, *51*, 6373−6377.
(19) Sun, Z.; Ni, W.; Yang, Z.; Kou, X.; Li, L.; Wang, J. Ph-Controlled Reversible Assembly and Disassembly of Gold Nanorods. *Small* **2008**, *4*, 1287−1292.
(20) Tian, Z.; Yang, C.; Wang, W.; Yuan, Z. Shieldable Tumor Targeting Based on Ph Responsive Self-Assembly/Disassembly of Gold Nanoparticles. *ACS Appl. Mater. Interfaces* **2014**, *6*, 17865−17876.
(21) He, H.; Feng, M.; Chen, Q.; Zhang, X.; Zhan, H. Light-Induced Reversible Self-Assembly of Gold Nanoparticles Surface-Immobilized with Coumarin Ligands. *Angew. Chem., Int. Ed.* **2016**, *55*, 936−940.
(22) Klajn, R.; Wesson, P. J.; Bishop, K. J.; Grzybowski, B. A. Writing Self-Erasing Images Using Metastable Nanoparticle "Inks. *Angew. Chem., Int. Ed.* **2009**, *48*, 7035−7039.
(23) Kundu, P. K.; Samanta, D.; Leizrowice, R.; Margulis, B.; Zhao, H.; Borner, M.; Udayabhaskararao, T.; Manna, D.; Klajn, R. Light-Controlled Self-Assembly of Non-Photoresponsive Nanoparticles. *Nat. Chem.* **2015**, *7*, 646−652.
(24) Liu, D.; Chen, W.; Sun, K.; Deng, K.; Zhang, W.; Wang, Z.; Jiang, X. Resettable, Multi-Readout Logic Gates Based on Controllably Reversible Aggregation of Gold Nanoparticles. *Angew. Chem., Int. Ed.* **2011**, *50*, 4103−4107.
(25) Das, S.; Ranjan, P.; Maiti, P. S.; Singh, G.; Leitus, G.; Klajn, R. Dual-Responsive Nanoparticles and Their Self-Assembly. *Adv. Mater.* **2013**, *25*, 422−426.
(26) He, L.; Hu, Y.; Kim, H.; Ge, J.; Kwon, S.; Yin, Y. Magnetic Assembly of Nonmagnetic Particles into Photonic Crystal Structures. *Nano Lett.* **2010**, *10*, 4708−4714.




DOI: 10.1021/acsnano.6b03396
*ACS Nano* 2016, 10, 7323−7330

(27) Wei, Y.; Han, S.; Kim, J.; Soh, S.; Grzybowski, B. A. Photoswitchable Catalysis Mediated by Dynamic Aggregation of Nanoparticles. *J. Am. Chem. Soc.* **2010**, *132*, 11018−11020.
(28) Cho, M. H.; Lee, E. J.; Son, M.; Lee, J. H.; Yoo, D.; Kim, J. W.; Park, S. W.; Shin, J. S.; Cheon, J. A Magnetic Switch for the Control of Cell Death Signalling in *in vitro* and *in vivo* Systems. *Nat. Mater.* **2012**, *11*, 1038−1043.
(29) Li, Z.; Zhu, Z.; Liu, W.; Zhou, Y.; Han, B.; Gao, Y.; Tang, Z. Reversible Plasmonic Circular Dichroism of Au Nanorod and DNA Assemblies. *J. Am. Chem. Soc.* **2012**, *134*, 3322−3325.
(30) Lu, Y.; Liu, J. Smart Nanomaterials Inspired by Biology: Dynamic Assembly of Error-Free Nanomaterials in Response to Multiple Chemical and Biological Stimuli. *Acc. Chem. Res.* **2007**, *40*, 315−323.
(31) Gurunatha, K. L.; Fournier, A. C.; Urvoas, A.; Valerio-Lepiniec, M.; Marchi, V.; Minard, P.; Dujardin, E. Nanoparticles Self-Assembly Driven by High Affinity Repeat Protein Pairing. *ACS Nano* **2016**, *10*, 3176−3185.
(32) Aili, D.; Gryko, P.; Sepulveda, B.; Dick, J. A.; Kirby, N.; Heenan, R.; Baltzer, L.; Liedberg, B.; Ryan, M. P.; Stevens, M. M. Polypeptide Folding-Mediated Tuning of the Optical and Structural Properties of Gold Nanoparticle Assemblies. *Nano Lett.* **2011**, *11*, 5564−5573.
(33) Coelho, J. P.; González-Rubio, G.; Delices, A.; Barcina, J. O.; Salgado, C.; Ávila, D.; Peña-Rodríguez, O.; Tardajos, G.; Guerrero-Martínez, A. Polyrotaxane-Mediated Self-Assembly of Gold Nanospheres into Fully Reversible Supercrystals. *Angew. Chem., Int. Ed.* **2014**, *53*, 12751−12755.
(34) Shiraishi, Y.; Shirakawa, E.; Tanaka, K.; Sakamoto, H.; Ichikawa, S.; Hirai, T. Spiropyran-Modified Gold Nanoparticles: Reversible Size Control of Aggregates by Uv and Visible Light Irradiations. *ACS Appl. Mater. Interfaces* **2014**, *6*, 7554−7562.
(35) Harimech, P. K.; Gerrard, S. R.; El-Sagheer, A. H.; Brown, T.; Kanaras, A. G. Reversible Ligation of Programmed DNA-Gold Nanoparticle Assemblies. *J. Am. Chem. Soc.* **2015**, *137*, 9242−9245.
(36) Kuzyk, A.; Schreiber, R.; Fan, Z.; Pardatscher, G.; Roller, E. M.; Hogele, A.; Simmel, F. C.; Govorov, A. O.; Liedl, T. DNA-Based Self-Assembly of Chiral Plasmonic Nanostructures with Tailored Optical Response. *Nature* **2012**, *483*, 311−314.
(37) Lu, F.; Yager, K. G.; Zhang, Y.; Xin, H.; Gang, O. Superlattices Assembled through Shape-Induced Directional Binding. *Nat. Commun.* **2015**, *6*, 6912.
(38) Chen, Q.; Whitmer, J. K.; Jiang, S.; Bae, S. C.; Luijten, E.; Granick, S. Supracolloidal Reaction Kinetics of Janus Spheres. *Science* **2011**, *331*, 199−202.
(39) Butt, H.; Graf, K.; Kappl, M. Surface Forces. In *Physics and Chemistry of Interfaces*; Wiley-VCH Verlag GmbH & Co. KGaA: Weinheim, 2004; pp 80−117.
(40) Wang, J.; Chen, S.; Cui, K.; Li, D.; Chen, D. Approach and Coalescence of Gold Nanoparticles Driven by Surface Thermodynamic Fluctuations and Atomic Interaction Forces. *ACS Nano* **2016**, *10*, 2893−2902.
(41) Li, X.; Zhou, L.; Wei, Y.; El-Toni, A. M.; Zhang, F.; Zhao, D. Anisotropic Encapsulation-Induced Synthesis of Asymmetric Single-Hole Mesoporous Nanocages. *J. Am. Chem. Soc.* **2015**, *137*, 5903−5906.
(42) Li, X.; Zhou, L.; Wei, Y.; El-Toni, A. M.; Zhang, F.; Zhao, D. Anisotropic Growth-Induced Synthesis of Dual-Compartment Janus Mesoporous Silica Nanoparticles for Bimodal Triggered Drugs Delivery. *J. Am. Chem. Soc.* **2014**, *136*, 15086−15092.
(43) Chen, G.; Wang, Y.; Yang, M.; Xu, J.; Goh, S.; Pan, M.; Chen, H. Measuring Ensemble-Averaged Surface-Enhanced Raman Scattering in the Hotspots of Colloidal Nanoparticle Dimers and Trimers. *J. Am. Chem. Soc.* **2010**, *132*, 3644−3645.
(44) Haiss, W.; Thanh, N. T. K.; Aveyard, J.; Fernig, D. G. Determination of Size and Concentration of Gold Nanoparticles from Uv−Vis Spectra. *Anal. Chem.* **2007**, *79*, 4215−4221.
(45) Ma, Y.; Li, W.; Cho, E. C.; Li, Z.; Yu, T.; Zeng, J.; Xie, Z.; Xia, Y. Au@Ag Core−Shell Nanocubes with Finely Tuned and Well-Controlled Sizes, Shell Thicknesses, and Optical Properties. *ACS Nano* **2010**, *4*, 6725−6734.
(46) Lee, Y. W.; Kim, M.; Kim, Z. H.; Han, S. W. One-Step Synthesis of Au@Pd Core−Shell Nanooctahedron. *J. Am. Chem. Soc.* **2009**, *131*, 17036−17037.
(47) Cang, H.; Labno, A.; Lu, C.; Yin, X.; Liu, M.; Gladden, C.; Liu, Y.; Zhang, X. Probing the Electromagnetic Field of a 15-Nanometre Hotspot by Single Molecule Imaging. *Nature* **2011**, *469*, 385−388.
(48) Yang, P.; Xu, Y.; Chen, L.; Wang, X.; Mao, B.; Xie, Z.; Wang, S. D.; Bao, F.; Zhang, Q. Encapsulated Silver Nanoparticles Can Be Directly Converted to Silver Nanoshell in the Gas Phase. *Nano Lett.* **2015**, *15*, 8397−8401.
(49) Zheng, Y.; Zhong, X.; Li, Z.; Xia, Y. Successive, Seed-Mediated Growth for the Synthesis of Single-Crystal Gold Nanospheres with Uniform Diameters Controlled in the Range of 5−150 nm. *Part. Part. Syst. Charact.* **2014**, *31*, 266−273.
(50) Hutter, E.; Boridy, S.; Labrecque, S.; Lalancette-Hébert, M.; Kriz, J.; Winnik, F. M.; Maysinger, D. Microglial Response to Gold Nanoparticles. *ACS Nano* **2010**, *4*, 2595−2606.


DOI: 10.1021/acsnano.6b03396
*ACS Nano* 2016, 10, 7323−7330